Pseudospin Quantum Hall Ferromagnetism

Yan Li
Department of Physics,University of Illinois at Urbana-Champaign

May 7, 2004

Abstract

Symmetry breaking ground states occur in quantum Hall effect (QHE) systems when two or more Landau levels become degenerate near the Fermi level. Isotropic, easy-axis or easy plane quantum Hall ferromagnets (QHF) can form depending on the pseudospins of the involved Landau levels consisting of real spin, orbit radius quantum number, subband index or growth direction. Theories based on Hartree-Fock calculation of pseudospin anisotropy energy are introduced, which classify the type of QHFs according to the nature of the degenerate Landau levels. Several representative experimental studies on the emergence of integer QHF in single-layer and double-layer two dimensional electron systems as well as of fractional QHF are presented. The anisotropy types are identified from the experimental measurements and compared with the prediction from the Hartree-Fock calculation. Discrepancy arises when neglected factors in the simple theoretical model become significant such as charge distribution profiles of different subbands, orbital effect of the in-plane magnetic field, softness of the barrier etc.

1 Introduction

Two dimension electron gas under a strong magnetic field is grouped into equally spaced energy levels known as Landau levels (LLs) with spacing $\Delta E = \hbar\omega_c = \hbar eB/m^*c$. Each LL has a degeneracy $N_\Phi = AB/\Phi_0$, where A is the system area and Φ_0 is the magnetic flux quantum $\Phi_0 = e/hc$. When the total number of electrons N is such that the filling factor $\mu = N/N_\Phi$ takes an integer or certain fractional values, quantum hall effects (QHE) occurs, characterized by a vanishing longitudinal resistance and a quantized transverse resistance. QHE provides a rich playground to study the many-particle collective phenomena, among which quantum Hall ferromagnetism (QHF) is a rather intriguing one and many exotic behaviors have been observed in experiments over different systems (1; 2; 3; 4; 5; 6).

When two LLs are brought to close affinity near the Fermi level and become nearly degenerate, e.g. by a tilted magnetic field in a single layer system, the competition of electrostatic energy and exchange energy leads the system to either isotropic, easy-axis or easy-plane ferromagnets (1; 7). *Easy-axis* (Ising) ferromagnets are systems with discrete directions along which the ordered states is energetically favored. for example, in the case of two degenerate LLs, if the exchange energy inside the same LL is stronger than that between different LLs, the total energy becomes lower if one of these aligned LLs is filled while the other one is left empty. The features of *easy-axis* anisotropy include long-range order at finite temperatures and Ising-like phase transitions. In contrast, *easy-plane* (XY) ferromagnets have a continuous set of pseudospin orientations in the plane, and the ordered states along any of them is an energy minimum. Due to the energy equality of these states, long-range order is absent while Kosterlitz-Thouless phase transition is possible at finite temperature. When there is no preferred direction for alignment to minimize the energy, the ferromagnets become *isotropic* and all possible directions of pseudospin have equal energy and there will be neither long-range order nor finite-temperature transition.

In this paper, a theoretical model based on Hartree-Fock calculation of pseudospin anisotropy energy is presented in Sec. 2, which predict the class of QHF systems with different pairs of crossing LLs. Then in Sec. 3, several recent experiments of QHF in single-layer, double-layer and fractional systems are reviewed, and the focus is laid upon the origin of spontaneous symmetry breaking of the ground state and the observed exotic behaviors related to the specific anisotropic class. Theoretical predictions are compared with experimental results and the limitation of the ideal-geometry HF model is discussed.

2 Theory of QHF classification

In the section, theories based on HF calculation of pseudospin anisotropy energy are presented(1; 7), which help understand how the competition between electrostatic and exchange energies determine the sign of the anisotropy energy and lead to *easy-axis* or *easy-plane* QHFs. For simplicity, it is assumed that only two LLs are nearly degenerate and the number of electrons is only enough to fill one of them.

2.1 Pseudospin orientation and anisotropy energy

Depending on the nature of the crossing LLs near the Fermi level, the pseudospin quantum number can involve degrees of freedom such as the real spins s, the orbital radius quantum number n, the subband index in a wide quantum well or the layer index of double or multiple quantum well ξ. Define the electronic states in the two involved LLs as pseudospin-up state $|\uparrow\rangle$ and pseudospin-down $|\downarrow\rangle$ state and in a pseudospin language(1; 8), the Hamiltonian of the system can be expressed as

$$\begin{aligned} H &= -b\sigma(\vec{q}=0) + \frac{1}{2A}\sum_{\vec{q}} \{V_{\rho,\rho}(\vec{q})\rho(-\vec{q})\rho(\vec{q}) + V_{\sigma,\sigma}(\vec{q})\sigma(-\vec{q})\sigma(\vec{q}) \\ &\quad + V_{\rho,\sigma}(\vec{q})\left[\rho(-\vec{q})\sigma(\vec{q}) + \sigma(-\vec{q})\rho(\vec{q})\right]\} \end{aligned} \tag{1}$$

where $\rho(\vec{q})$ and $\sigma(\vec{q})$ are the sum and difference operators projected onto up and down states and $V_{ss'}$ are the corresponding effective interactions. b is the half of the $s$ingle particle energy separation of the nearly degenerate LL's.

Assume that the many-particle ground state is fully polarized along direction $\hat{n} = (\sin\theta\cos\phi, \sin\theta\sin\phi, \cos\theta)$ and can be described by the single Slater determinant wave function (1):

$$|\Phi_{\hat{n}}\rangle = \prod_{m=1}^{N_\Phi} c^+_{m,\hat{n}}|0\rangle, \tag{2}$$

where m is the orbital index within a LL. The energy of the ground state can be estimated by $E_{GS} = \langle\Psi_{\hat{n}}|H|\Psi_{\hat{n}}\rangle/N$. By mapping the wave function and Hamiltonian onto the space spanned by the pseudospins and keeping only those terms dependent of the pseudospin orientations, we get the ground state energy(1):

$$\begin{aligned} E_{GS} &= -(b - U_{\rho,\sigma})\cos\theta + \frac{U_{\sigma\sigma}}{2}\cos^2\theta \\ U_{s,s'} &= \int \frac{d\vec{q}}{(2\pi)^2}[V_{s,s'}(\vec{q}=0) - V_{s,s'}(\vec{q})]\exp(-q^2l^2/2), \end{aligned} \tag{3}$$

where $l = \sqrt{\hbar c/eB}$ is the magnetic length. Let us have a close look of the terms involved in the ground state energy:

1. The **effective symmetry breaking field** $b^* = b - U_{\rho,\sigma}$ include both external and internal components. b in general includes external bias potential (Δ_V), tunneling barrier energy (Δ_t), LL spacing ($\hbar\omega_c$), Zeeman splitting energy ($g^*\mu_B B$) and contributions from lower lying LL's (I_0), depending on the nature of the two crossing LL's. $U_{\rho,\sigma}$, determined from $V_{\rho,\sigma} = (V_{\uparrow,\uparrow} - V_{\downarrow,\downarrow})/4$, is the contribution to the symmetry-breaking field resulting from the Coulomb interaction difference of electrons in the two LLs.

2. The sign of the **anisotropic energy** $U_{\sigma,\sigma}$ is determined from $V_{\sigma,\sigma} = (V_{\uparrow,\uparrow} + V_{\downarrow,\downarrow} - 2V_{\downarrow,\uparrow})/4$ and consists of two competing terms. The electrostatic Coulomb interaction $V_{\sigma,\sigma}(\vec{q}=0)$ is non-vanishing when the two pseudospins have different charge density distribution perpendicular to the electron plane. This term is usually orientation-independent, and thus favors easy-plane anisotropy. $V_{\sigma,\sigma}(\vec{q})$ is the exchange penalty for flipping the pseudospin orientation and thus favors easy-axis anisotropy.

3. The **pseudospin orientation** can be determined by minimizing E_{GS} in Eqn.(3) and is plotted as a function of the dimensionless field $u = b^*/|U_{\sigma,\sigma}|$ at positive and negative $U_{\sigma,\sigma}$ respectively in Fig. 1. When $U_{\sigma,\sigma} > 0$, the pseudospin changes continuously with the field when $|u| < 1$ and reached alignment at $u > 1$ ($\theta = 0$) or $u < -1$ ($\theta = \pi$). Since E_{GS} is independent of in-plane angle ϕ, according to our definition in Sec.1, this case corresponds to *easy-plane* anisotropy. When $U_{\sigma,\sigma} < 0$, there is two energetically unequal local minimum at $\theta = 0$ and $\theta = \pi$, which results in *easy-axis* anisotropy. If a barrier separate these two states, hysteric behavior will appear when swapping the field upward and downward. A situation not shown in Fig. 1 is when $U_{\sigma,\sigma} = 0$, which correspond to spontaneous symmetry breaking to an *isotropic* state in absence of effective field b^*.

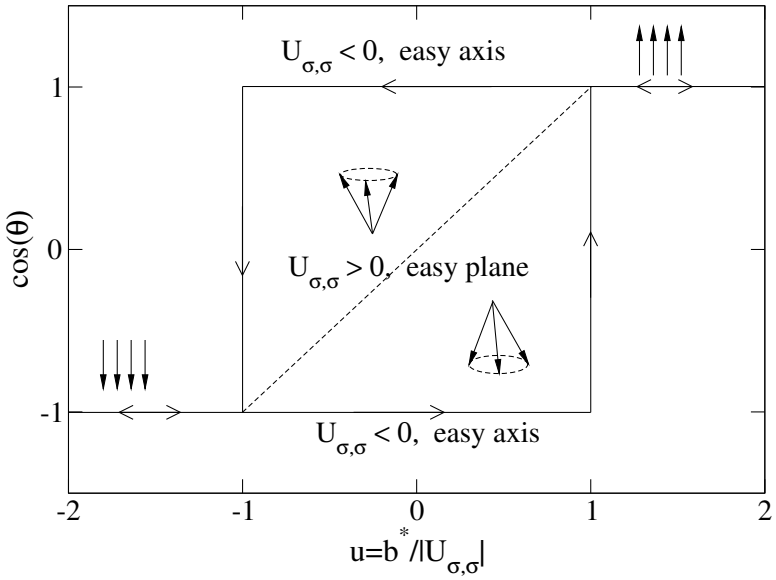

Figure 1: The value of $\cos\theta$ that minimize the ground state energy in Eqn.(3) as a function of the dimensionless field $u = b^*/|U_{\sigma,\sigma}|$ for $U_{\sigma,\sigma} > 0$ (i.e.easy-plane anisotropy, dashed line) and $U_{\sigma,\sigma} < 0$ (i.e. easy-axis anisotropy, solid line) cases. Also shown is the schematics of corresponding pseudospin orientation.

A more complete description of the many-body Hamiltonian and HF total energy can be found in Ref.(7), with detailed derivation of pseudospin matrix elements of Coulomb interaction for different situations of LL's crossing. Since the spirit of the anisotropy energy calculation is the same, I won't repeat the lengthy derivations here but instead use the their conclusions about the classification of QHF types for particular pairs of crossing LLs in the following.

2.2 Classification of QHFs

The nature of the LL's crossing can be represented by the a set of quantum number $\{\xi_{1,2}, s_{1,2}, n_{1,2}\}$, which are the subband index, spin index and orbital radius quantum number of the two pseudospin states respectively, determined by the system geometry and external conditions. The

HF anisotropy energy calculation (7) is carried out in an idealized system consisting of two nearby infinitely narrow 2D layers separated by a distance d. With a tunneling barrier Δ_t and external bias Δ_V, the single-particle of quantum numbers $\{\xi = \pm 1, s = \pm 1/2, n\}$ can be expressed as :

$$E_{\xi,n,s} = -\frac{\xi}{2}(\Delta_V^2 + \Delta_t^2)^{1/2} + \hbar\omega_c(n + \frac{1}{2}) - s|g|\mu_B B \tag{4}$$

Quantum hall ferromagnetism occurs when two LLs are brought to nearly alignment. Define the two levels as pseudospin up $|\uparrow\rangle$ and pseudospin down $|\downarrow\rangle$, and a state with the pseudospin oriented to a direction $\hat{m} = (\sin\theta\cos\phi, \sin\theta\sin\phi, \cos\theta)$ can be mapped onto them as:

$$|\hat{m}\rangle = \cos\left(\frac{\theta}{2}\right)|\uparrow\rangle + \sin\left(\frac{\theta}{2}\right)e^{i\phi}|\downarrow\rangle. \tag{5}$$

The pseudospin orientation of the ground state is determined by minimizing the HF ground state energy (7):

$$E_{HF}(\hat{m}) = \langle\hat{m}|H|\hat{m}\rangle/N = \sum_{i=x,y,z} b^* m_i + \frac{1}{2}\sum_{i,j=x,y,z} U_{i,j} m_i m_j \tag{6}$$

and the type of QHF is determined by the sign of the anisotropy energy $U_{i,j}$, which in turn depends on the nature of the nearly degenerate LLs.

2.2.1 Two LLs within the same subband: $\xi_1 = \xi_2$

Within the same subbands, the two nearly aligned LLs must have opposite real spins because LLs with same real spin are always separated by multiples of $\hbar\omega_c$. Since the charge distributions of these two pseudospns only differ *in the plane*, the electrostatic terms vanish and the only nonzero contribution to the anisotropy energy (7) is from the exchange energy:

$$U_{z,z} = -\frac{1}{8}\int_0^\infty dq e^{-q^2/2}[L_{n_1}(q^2/2) - L_{n_2}(q^2/2)]^2[(1 + r_\Delta^2) + (1 - r_\Delta^2)e^{-dq}] \tag{7}$$

where $L_n(x)$ is the Laguerre polynomial and $r_\Delta = \Delta_V/(\Delta_V^2 + \Delta_t^2)^{1/2}$. When the orbital radius quantum numbers are the same ($n_1 = n_2$), $U_{z,z} = 0$ and the QHF state is *isotropic*. Since the only different quantum number of the two pseudospins is the sign of real spins, the *isotropic* anisotropy indicate the independence of the Coulomb interaction on real spins. One example is $n_1 = n_2 = 0$ and $r_\Delta = 1$ (i.e. $\Delta_t \to \infty$, no tunneling), which is reduced to the well studied single-layer isotropic $\nu = 1$ QHFs (9). By techniques such as tilted magnetic fields, the Zeeman splitting ($\sim |B_{tot}|$) can be made larger than the cyclotron energy $\hbar\omega(\sim B_z)$ and $n_1 \neq n_2$ can be realized. In that case, $U_{z,z}$ is always negative in Eqn. (7) and results in *easy-axis* anisotropy. Again when $r_\Delta = 1$, it reduces to a single-layer 2D system, which will be illustrated in Sec. 3.

2.2.2 Two LLs in different subbands: $\xi_1 \neq \xi_2$

There are more possible combinations of different quantum numbers when the involved two LLs have different subband indices $\xi_1 \neq \xi_2$. First, let's look at the case that the orbital radius quantum number $n_1 = n_2$.

1. $n_1 = n_2$

   (a) Since the two LLs are from different subbands (layers), their real spins can be same of opposite. If $s_1 = s_2$, the only nonzero anisotropy energy terms and the HF energy in the absence of effective symmetry-breaking fields are (7):

$$\begin{aligned} U_{z,z} &= u r_\Delta^2; \quad U_{x,x} = u(1 - r_\Delta^2) \\ U_{x,z} &= U_{z,x} = (U_{z,z} U_{x,x})^{1/2} \\ E_{HF} &= \sum_{i,j=x,y,z} U_{i,j} m_i m_j = u[r_\Delta m_z + (1 - r_\Delta^2)^{1/2} m_x] \end{aligned} \tag{8}$$

   where u is a positive constant. It's easy to see that the HF energy E_{HF} is minimized to zero by condensing the pseudospins onto the plane tilted from the $X-Y$ plane by an angle $\cos^{-1} r_\Delta$, leading to *easy-plane* anisotropy, i.e. interlayer coherence.

   (b) If the two LLs have opposite spins, $s_1 = -s_2$, then $U_{x,x}$, $U_{x,z}$ and $U_{z,x}$ all vanish because they involve pseudospin non-conserving scattering processes. Since $U_{z,z} = u r_\Delta^2 \geq 0$, the system is *isotropic* when $r_\Delta = 0$ (i.e. no bias) and *easy-plane* otherwise. Note that $\xi_{1,2}$ could be the indices of two separated layers in a double-quantum-well 2D system (3) or of two layers separated by a soft barrier in a wide single-quantum well (4). In the latter case, Δ_t also depends on the pseudospin orientation as will be shown in Sec. 3, and first-principle calculation shows that *easy-axis* and *easy-plane* QHF are favored at low and high electron density respectively (4).

2. $n_1 \neq n_2$

   Finally, let's look at the case that $\xi_1 \neq \xi_2$ and $n_1 \neq n_2$.

   (a) When $s_1 = s_2$, the only non-vanishing anisotropy energy terms are $U_{z,z}$ and $U_{y,y} = U_{x,x}$, all as functions of the layer separation d and r_Δ. The HF total energy can be written as (7):

$$E_{HF} = \sum_{i,j=x,y,z} U_{i,j} m_i m_j = (U_{z,z} - U_{x,x}) m_z^2 + U_{x,x}, \tag{9}$$

   thus the QHF will have *easy-plane* anisotropy when $U_{z,z} - U_{x,x} > 0$ and *easy-axis* anisotropy when $U_{z,z} - U_{x,x} > 0$. When the layer separation takes a critical value d^* so that $U_{z,z} - U_{x,x} = 0$, the QHF is *isotropic*.

   (b) Again, when $s_1 \neq s_2$, only $U_{z,z}$ remains nonzero and the type of the QHF is determined by the sign of $U_{z,z}$ at particular d and r_Δ.

One important message here is that when the subband wave functions are different, the pseudospin anisotropy can be vary in the $r_\Delta - d$ plane. Thus phase transitions between QHFs are possible by carefully tuning the external parameters (7).

3 Experiments on quantum Hall ferromagnetism

In this section, I will review several representative experiments on QHF in different systems, including single-layer and bilayer quantum well systems and fractional systems. Exotic phenomena related to the *easy-axis* and *easy-plane* QHF, such as unusual magnetotrasnport observations, anomalous temperature dependence of longitudinal resistance etc. are presented. Physical origins for the emergence of the pseudospin anisotropy are discussed and compared with theories presented in Sec. 2. Experimental setup and realization of LL degeneracy (crossing) by adjusting control parameters are also mentioned.

3.1 Single-layer 2D electron system

Measurements of integer quantum Hall effect in single-layer 2D electron system is carried out in a 43nm wide unbalance GaAs quantum well at T=300mK (1). The tilted magnetic field technique is used to align two LLs with *opposite* spins at even filling number $\nu = 2, 4$ (see Fig. 2). The pseudospin are $\{\xi_1 = \xi_2, s_1 = -s_2, n_1 \neq n_2\}$ and according to results in Sec. 2.2.1 both cases should result in *easy-axis* anisotropy QHF.

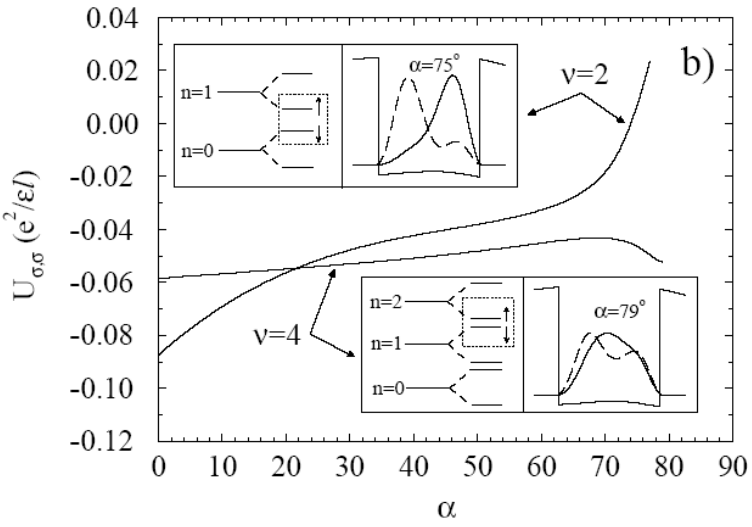

Figure 2: The anisotropy energy $U_{\sigma,\sigma}$ (see definition in Sec. 2.1) by LDA calculation as a function of the tilted angle α for $\nu = 2$ and $\nu = 4$. Also shown are the density profiles for up (dashed line) and down (solid line) pseudospin orbitals at large α (1).

Indeed, in the experiments, the $\nu = 4$ quantum Hall effect, i. e. the minimum of longitudinal resistance is lost near the predicted tilting angle $\alpha = 79°$ at which the two involved LLs become degenerate, which can be associated with the *easy-axis* anisotropy(1). This is in agreement with the LDA calculated anisotropy energy $U_{\sigma,\sigma}$ for $\nu = 4$ in Fig. 2, which is only weakly dependent of α and always negative, i. e. favoring *easy-axis* anisotropy. However, for $\nu = 2$, no loss of quantum Hall effect is observed around the predicted tilting angle $\alpha = 75°$ of LLs alignment, consistent with the *easy-plane* anisotropy. This is also confirmed from the positive value of $U_{\sigma,\sigma}$ for $\nu = 2$ at large α in Fig. 2. The discrepancy

with theory in Sec. 2.2.1 is due to the fact in Eqn.(7) a *zero-width* quantum well model is assumed. In a *finite width* quantum well, the orbital effect of the in-plane magnetic field and the electrostatic contribution from the different charge density profile of the two LLs can't be neglected and thus the sign of $U_{\sigma,\sigma}$ depends not only on the system geometry but also the tilting angle and the filling factor. That explains why different QHF behavior occurs for $\nu = 2$ and $\nu = 4$, even their pseudospin configuration fall in the same category.

3.2 Double-layer 2D electron system

Now let us turn to the case of double-layer systems, i.e. $\xi_1 \neq \xi_2$. This can be realized a double quantum well, a wide unbalance single quantum well or a thin symmetric single quantum well , as illustrated by the following examples. As we shall see, different types of QHF occur due to the different geometry and nature of electron-electron interaction.

3.2.1 Example 1: phase transition in $\nu = 2$ double quantum well

The sample consists of two modulation doped GaAs quantum wells of width of 20nm separated by an $Al_{0.3}Ga_{0.7}As$ barriers of thickness 3.1nm (3). A magnetic field $B \leq 13.5$T is applied perpendicular to the electron layer. The total electron density n_t and the front-back density different $n_f - n_b$ are controlled independently by adjusting the gate voltage at the front and back gate electrodes.

The transverse Hall resistance and the activation energy are measured at different electron density difference $n_f - n_b$ and total density n_t. It is concluded that the $\nu = 2$ QH state undergoes a phase transition from a compound (spin polarized) state to a coherent state (unpolarized) when n_t decreases or $|n_f - n_b|/n_t$ increases.

The emergence of the coherence state at $\nu = 2$ is explained by dominance of the interlayer Coulomb interaction over the intralayer Coulomb interaction, which enhance the interlayer correlation and support coherence state. In a pseudospin language, the up and down pseudospins belong to different layers and when $\nu = 2$, the real spins of the two LLs are of opposite sign. Comparing with theory in Sec. 2.2.2, the experimental observation agrees with the prediction of *easy-plane* pseudospin QHF for the case $\xi_1 \neq \xi_2, n_1 = n_2(= 0), s_1 = -s_2$.

3.2.2 Example 2: First-order phase transition in $\nu = 2, 4$ single quantum well

The sample is a 60 nm wide gallium arsenide quantum well under a perpendicular magnetic field (4). An electric field is applied across the sample through the evaporated gate electrode to change the electron density and the energy separating of the involved LLs so that different pairs of LLs can be aligned. The difference from the double quantum well in example 1 is that here we have a wide *single* quantum well and the two "layers" are separated by a *soft* barrier originating from the Coulomb interactions among electrons in the quantum well. Here "layer" indices are used to indicate LLs that occupies dominantly the left or the right side of the well.

Transverse resistivity for $\nu = 2$ and $\nu = 4$ are measured and the suppression of quantum Hall effect is observed when two LLs from different "layers" are aligned at the Fermi level (see Fig. 3). This is found to be strongly correlated with the appearance of hysteresis in ρ_{xx}

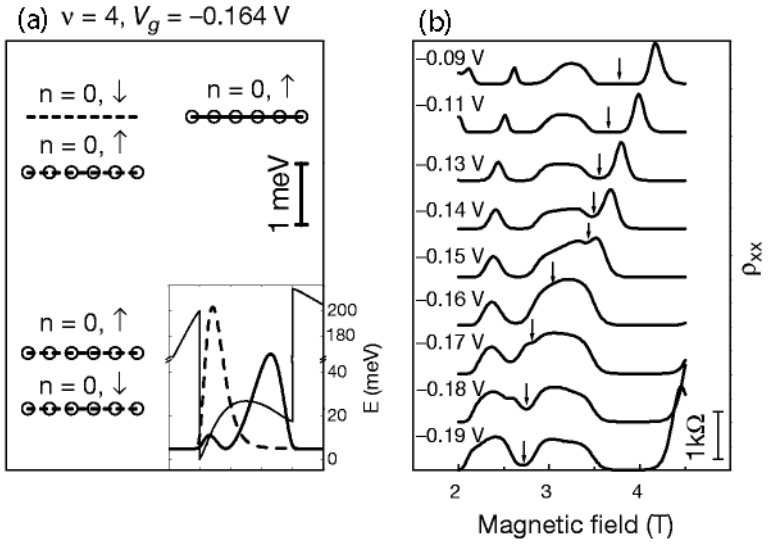

Figure 3: (a) LDA calculation of energy spectrum of $\nu = 4$ at $V_g = -0.164$ V, where the two LLs $\{L, n = 1, s = \uparrow\}$ and $\{R, n = 0, s = \downarrow\}$ are aligned (typos in the original figure ?). Circles and dashed lines indicate occupied and empty states. Inset show LDA quantum well profile and wave functions. (b) Longitudinal resistivity ρ_{xx} as a function of magnetic field at $\nu = 4$ at $T = 330$ mK shows the disappearance of Quantum Hall states (marked by arrows) (4). Similar phenomena are observed for the case of $\nu = 2$.

when the magnetic field is swept up and down. The hysteresis disappears at about 1K and the measured temperature dependence of the hysteric behavior indicate the characteristic energy is about the scale of the electron-electron interaction(4).

The appearance of hysteresis is attributed to occurrence of *easy-axis* (Ising-like) QHF, which imposes an energy barrier to flip the pseudospin, causing a first-order phase transition between oppositely polarized ($\theta = 0, \pi$) ground states. Notice that theory predict a *isotropic* QHF for a bilayer system with a rigid tunneling barrier for the case of $\xi_1 \neq \xi_2, n_1 = n_2, s_1 = -s_2$, when the two LLs are aligned ($r_\Delta = 0$). However, in the experiments, $\nu = 2$ state turns out to be of *easy-axis* anisotropy just as $\nu = 4$ state. The difference is caused by the softness of the barrier separating left and right "layers". LDA calculation predicts that at sufficiently high electron density, the tunneling gap between the filled state and the empty state at the Fermi level is enhanced and it becomes energetically more favorable for the system to behave like an Ising ferromagnet. For odd filling factor, experiments observation agrees with the *easy-plane* QHF just as predicted by theory for the case $\xi_1 \neq \xi_2, n_1 = n_2, s_1 = s_2$.

3.2.3 Example 3: *easy-axis* and *easy-plane* QHF in a symmetric quantum well

The experiment is performed on a 40nm wide GaAs single-quantum well (6). The charge density n_s is varied by the front and back gate to make the LL crossing occur at desired filling factor while the quantum well potential is always kept *symmetric*. In this case, the pseudospins of the involved LLs are either symmetric or antisymmetric about the quantum well and are labeled by $\{\xi = S/A, n, s\}$. The corresponding wave function and energy

spectrum are shown in Fig. 4 (a), (b). The energy difference of up and down pseudospins is:

$$\Delta_Z = \left[|\Delta n| \frac{\hbar e}{m^*} + \Delta s |g| \mu_B - \left(\frac{\partial \Delta_{SAS}}{\partial n_s} \right) \frac{\nu e}{h} \right] \tag{10}$$

where the energy separation of symmetric and anti-symmetric state Δ_{SAS} decreases with increasing n_s. Since these two subbands are distinguished by their symmetry instead of by the separation of a distance d as in the double quantum well case, the conclusions in Sec.2.2 cannot be applied directly.

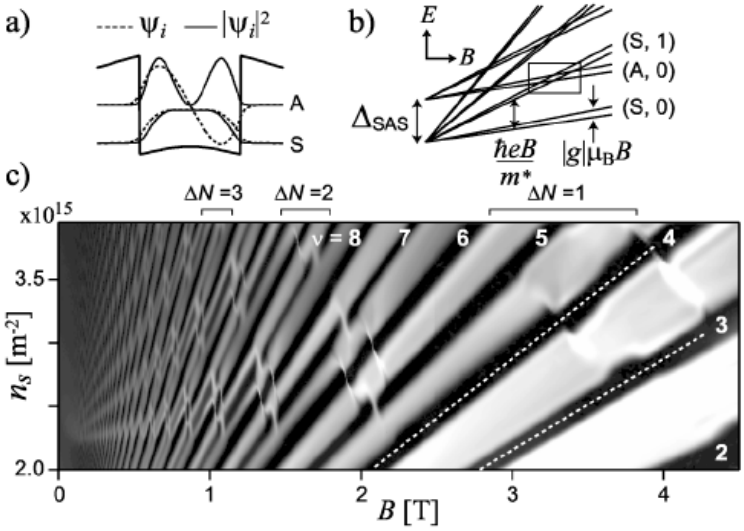

Figure 4: (a)Calculated wave function and charge density distribution for the symmetric quantum well. (b) LL energy diagram and level crossings at $\nu = 3, 4$ are shown in the box. (c) Gray-scale plot of R_{xx} at 50 mK. Dark regions represent small values of R_{xx} (6).

The transverse resistance R_{xx} is measured at different point in the n_s, B space as shown in Fig. 4(c). At $\nu = 3$ region, where $\{S, 1, \uparrow\}$ and $\{A, 0, \uparrow\}$ are aligned and the quantum Hall region evolves smoothly around the field where the two LLs cross ($B \sim 3.9$T), implying *easy-plane* anisotropy. This is explained by the fact that up and down pseudospin states have symmetric and anti-symmetric charge distribution perpendicular to the electron plane and it is energetically favorable to mix these two states and condense the pseudospin onto the X-Y plane. In contrast, the center $\nu = 4$ quantum Hall region jumps vertically, corresponding to a *easy-axis* anisotropy. In this case, $\{S, 1, \downarrow\}$ and $\{A, 0, \uparrow\}$ are aligned and due to their different sign of real spin, the exchange energy dominates and impose a penalty to flip the pseudospin, resulting in either up or down magnetization.

3.3 Fractional system

Finally, I want to mention some recent experiments of QHF in a fractional quantum Hall system (2; 5). The sample is a high-quality GaAs/AlGaAs heterostructure and hydrostatic pressure about 10 Kbar is applied to study the evolution of $\nu = 2/5$ quantum Hall state. At

high pressure, the unpolarized state and polarized state compete with each other, leading to a coexistence over a large range of pressure. These nearly degenerate states can be mapped on to the pseudospin up and down sates and at certain pressure, the system is turned into polarized state with the emergence of hysteric transport (see Fig. 5) and anomalous temporal relaxation of the transverse resistivity (5), indicating *easy-axis* anisotropy. The theory in Sec. 2 can be extended here in the fractional quantum hall regime under the composite Fermion picture.

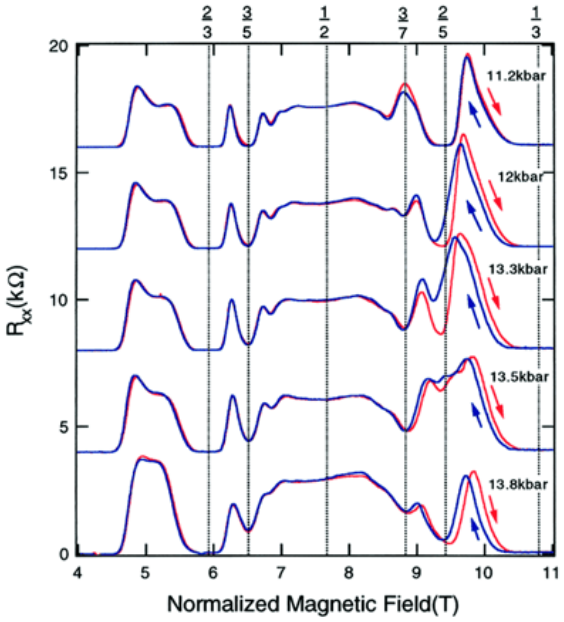

Figure 5: Magneto-resistance of a high-quality GaAs/AlGaAs heterostructure at 40 mK of temperature under pressure near filling fraction $\nu = 2/5$. Arrows indicate the sweep direction.

Summary

In this paper, theories and experiments on integer and fractional quantum Hall ferromagnets are briefly reviewed. A theoretical model for quantum Hall ferromagnets based on Hartree-Fock energy calculation is introduced and results about QHF classification are presented. This model qualitatively explains the physical origin of the emergence of *isotropic, easy-axis* and *easy-plane* anisotropy in QHFs. The predicted anisotropy types for different nature of LL crossing agree with most experiments, while the discrepancy can be accounted for by the neglected factors in the theoretical model such as the nature of the tunneling barrier, coupling between the external field and internal degrees of freedoms etc. As suggested by both theory and experiments, phase transitions from one type of QHF to another type can be made possible by varying the external parameters.

References

[1] T. Jungwirth, S. P. Shukla, L. Smrčka, M. Shayegan, and A. H. MacDonald. *Phys. Rev. Lett.*, 81:2328–2331, 1998.

[2] H. Cho, J. B. Young, W. Kang, K. L. Campman, A. C. Gossardand M. Bichler, and W. Wegscheider3. *Phys. Rev. Lett.*, 81:2522–2525, 1998.

[3] A. Sawada, Z. F. Ezawa, H. Ohno, Y. Horikoshi, Y. Ohno andS. Kishimoto, F. Matsukura, M. Yasumoto, and A. Urayama. *Phys. Rev. Lett.*, 80:4534–4537, 1998.

[4] Vincenzo Piazza, Vittorio Pellegrini, Fabio Beltram, Werner Wegscheider TomÁ Jungwirth, and Allan H. MacDonald. *Nature*, 402:638–641, 1999.

[5] J. Eom, H. Cho, W. Kang, K. L. Campman, A. C. Gossard, M. Bichler, and W. Wegscheider. *Science*, 289:2320–2323, 2000.

[6] Koji Muraki, Tadashi Saku, and Yoshiro Hirayama. *Phys. Rev. Lett.*, 87:196801–196804, 2001.

[7] TomÁ. Jungwirth and Allan. H. MacDonald. *Phys. Rev. B*, 63:035305–035314, 2000.

[8] A. H. MacDonald, P. M. Platzman, and G. S. Boebinger. *Phys. Rev. Lett.*, 65:775–778, 1990.

[9] S. M. Girvin. *Physics Today*, 53:39–45, 2000.